

DCCT DIAGRAM OF A CASE-HARDENING STEEL 20MnCrS5

¹Michal KONDERLA, ¹Ivo SCHINDLER, ²Zdeněk SOLOWSKI, ¹Tomáš MERVA, ¹Svatopluk ČECH

¹VŠB - Technical University of Ostrava, Faculty of Materials Science and Technology, Ostrava,
Czech Republic, EU, michal.konderla.st@vsb.cz

²TŘINECKÉ ŽELEZÁRNY a.s., Třinec, Czech Republic, EU, Zdenek.Solowski@trz.cz

<https://doi.org/10.37904/metal.2023.4691>

Abstract

Grade 20MnCrS5 is a structural alloy steel for surface hardening. Despite the low carbon content, it exhibits good wear resistance after hardening. The material can be hardened to a depth of about 40 mm. Sulphur in the content of 0.020 - 0.040 % improves lubricant function during cold processing. The material is commonly used for the production of moderately stressed parts of motor vehicles and machine parts intended for cementation with higher strength in the core (e.g. transmission gears, axles, pinions and camshafts). Continuous cooling transformation diagram of steel grade 20MnCrS5 was constructed after the compressive true strain of 0.35 with the strain rate of 1 s^{-1} . Based on the experimentally determined value of $A_{c3} = 829 \text{ }^{\circ}\text{C}$, the austenitization temperature of the dilatometric samples was chosen to be $880 \text{ }^{\circ}\text{C}$. Samples cooled at a constant nominal rate of $0.1\text{-}35 \text{ }^{\circ}\text{C}\cdot\text{s}^{-1}$ were subjected to structural analyses (optical and scanning microscopy) as well as hardness measurements. Even at the highest applied cooling rate, trace amounts of ferrite were detected. Martensite and bainite appeared in the structure after cooling at a rate of at least $0.7 \text{ }^{\circ}\text{C}\cdot\text{s}^{-1}$. Continuous cooling transformation diagrams are valuable from the point of view of optimizing the cooling regimes after hot bulk forming and/or at the heat treatment of the final products.

Keywords: Low-alloy Cr-Mn steel, DCCT diagram, dilatometry, microstructure, SEM

1. INTRODUCTION

Important steel parts for the automotive industry, such as gearboxes, pinions, camshafts and overrunning clutch, are produced from low-alloy manganese-chromium steels. The working surface of these components is highly stressed due to abrasion. Steel 20MnCrS5 is intended for surface cementation of parts. For steels with a low carbon content of up to 0.30 %, the surface becomes saturated with carbon at elevated temperatures in an environment with a high carbon concentration. After subsequent quenching, a very wear-resistant layer formed by components such as martensite is achieved [1]. The blanks for the production of these components are produced by rolling. By controlled cooling, the effort is to achieve a well-machinable ferritic-pearlitic structure. Knowledge of continuous cooling transformation (CCT) diagrams plays a key role in this. The type and kinetics of individual phase transformations are mainly influenced by the chemical composition of the steel [2-4], initial grain size [5,6] and pre-deformation [7,8]. The aim of the work was to develop the DCCT diagram (i.e. with the influence of previous deformation) of steel 20MnCrS5 with 0.20 % C; 1.27 % Mn; 0.24 % Si; 0.015 % P; 0.027 % S; 1.26 % Cr; 0.21 % Ni; 0.028 % Al; 0.015 % Mo; 0.011 % N. The results will help in the controlled cooling of rods and coils of rods.

2. EXPERIMENTAL PROCEDURES

The test material was prepared in the form of hot-rolled rods with a diameter of 12 mm. Dilatometric samples with a diameter of 6 mm and a length of 86 mm were made by cutting and turning. Experimental work was based on a combination of dilatometric tests (performed using a non-contact optical scanning system on a hot

deformation simulator Gleeble 3800-GTC), metallographic analyzes and hardness measurements of samples after dilatometry (all at the center of the cross-section). To determine the appropriate austenitization temperature, a dilatometric test was performed with slow heating at a rate of $0.167\text{ }^{\circ}\text{C}\cdot\text{s}^{-1}$. The obtained dilatometric curve was numerically derived in the mathematical software Origin (OriginLab) and the phase transformation temperatures $A_{c1} = 741\text{ }^{\circ}\text{C}$ and $A_{c3} = 829\text{ }^{\circ}\text{C}$ were determined (**Figure 1**). With regard to the technological possibilities of rolling in operating conditions, the austenitization temperature of the dilatometric samples was determined to be $880\text{ }^{\circ}\text{C}$.

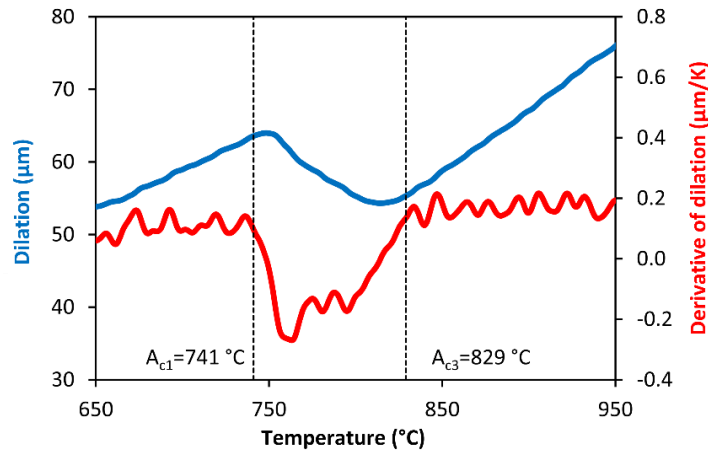
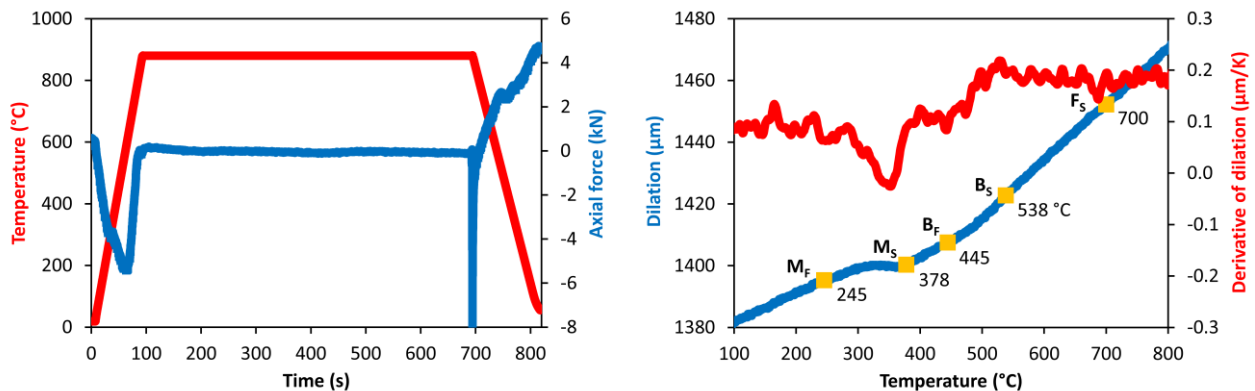


Figure 1 Determination of transformation temperatures during slow heating

The dilatometric samples were resistively heated in the measured zone at a rate of $10\text{ }^{\circ}\text{C}\cdot\text{s}^{-1}$ to the chosen austenitization temperature and, after holding for 600 s, deformed by uniaxial compression at a rate of 1 s^{-1} to the true strain of 0.35. Immediately afterwards, they were cooled at selected constant rates (i.e. nominally $0.1\text{--}35\text{ }^{\circ}\text{C}\cdot\text{s}^{-1}$). The registered dilatometric curves were analyzed using the special CCT software (DSI) and the mathematical program Origin (OriginLab). **Figure 2** shows an example of a dilatation curve and its additional analysis using numerical derivation.



a) time course of the dilatometric test

b) analysis of the dilatation curve

Figure 2 Example of data obtained by dilatometry (cooling rate of $7.0\text{ }^{\circ}\text{C}\cdot\text{s}^{-1}$)

The temperatures and types of phase transformations determined in this way were verified in all cases by metallographic analyzes using optical microscopy, or by measuring the hardness. In selected cases, the minor phase components were verified using SEM-SEI electron microscopy. Microstructures in **Figures 3** and **4** document the effect of cooling rate on the resulting microstructure (F = ferrite, P = pearlite, B = bainite, M = martensite).

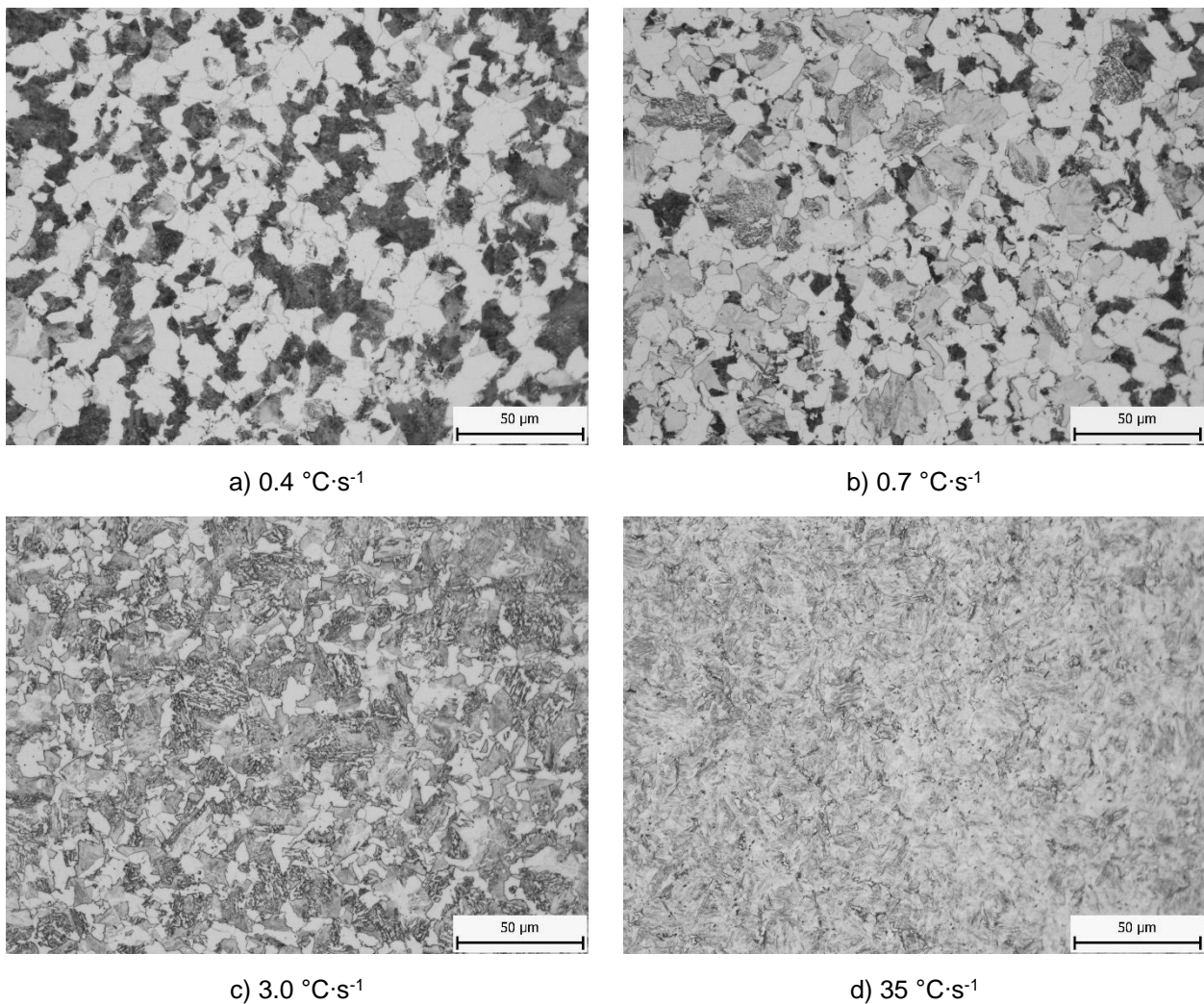


Figure 3 Effect of cooling rate on the final microstructure (optical microscopy)

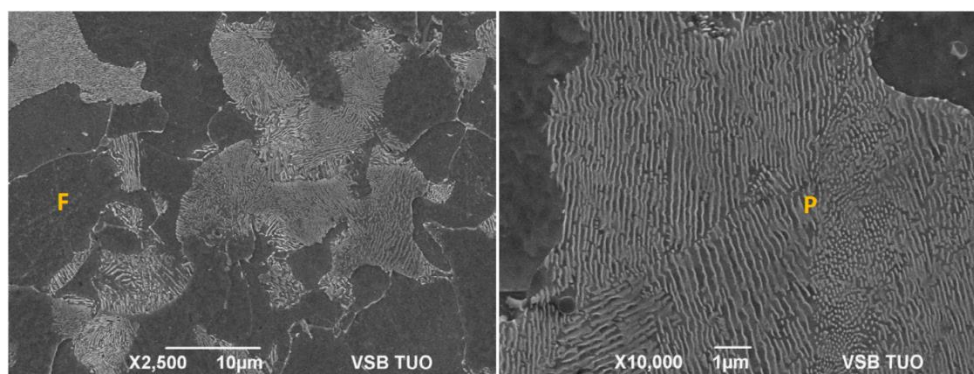
3. DISCUSSION OF RESULTS

Cooling at the lowest rates (up to $0.4 \text{ } ^\circ\text{C}\cdot\text{s}^{-1}$) led to the formation of ferrite and pearlite. As the cooling rate increases, the proportion of hard components, i.e. bainite and martensite gradually increases. Even at the fastest possible cooling (i.e. $35 \text{ } ^\circ\text{C}\cdot\text{s}^{-1}$), ferrite was present in at least a trace amount in the structure. The hardness of the selected samples was measured by the Brinell method and then converted to HV 30 hardness (according to Vickers). A carbide ball with a diameter of 2.5 mm was pressed into the material with a force of 1,839 N. Each sample was tested three times in the central area of the cross section; the average hardness values are given in the **Table 1** which simultaneously documents the phase components identified by metallographic analysis. From left to right, the phase fractions are listed in decreasing amount. A small fraction is given in round brackets and a trace amount of the given phase component in square brackets.

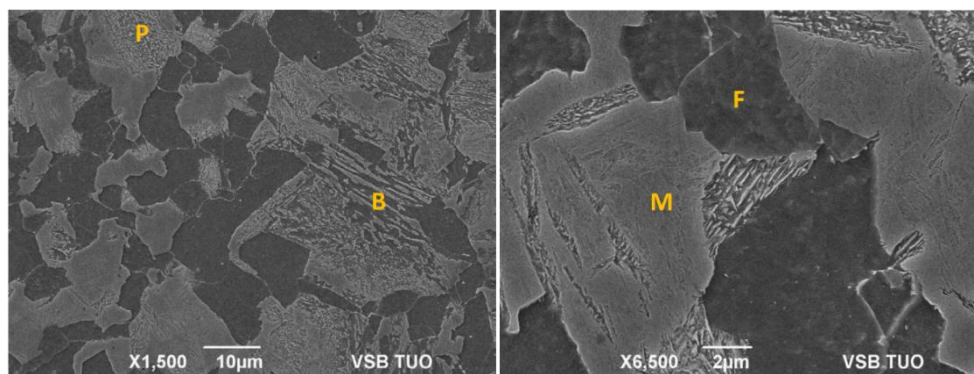
The trend of the measured hardness is documented in **Figure 5**. Growth of hardness after cooling at a rate greater than $0.4 \text{ } ^\circ\text{C}\cdot\text{s}^{-1}$ signals the an ever-increasing share of martensite and bainite. Based on the three types of results described above, it was possible to compile a DCCT diagram of 20MnCrS5 steel after austenitization and deformation realized at a temperature of $880 \text{ } ^\circ\text{C}$ (see **Figure 6a**). From this diagram, the temperatures of the start and finish of individual phase transformations can be read, as well as the limiting cooling rates for the corresponding phase regions.

Table 1 Effect of cooling rate on phase composition and hardness

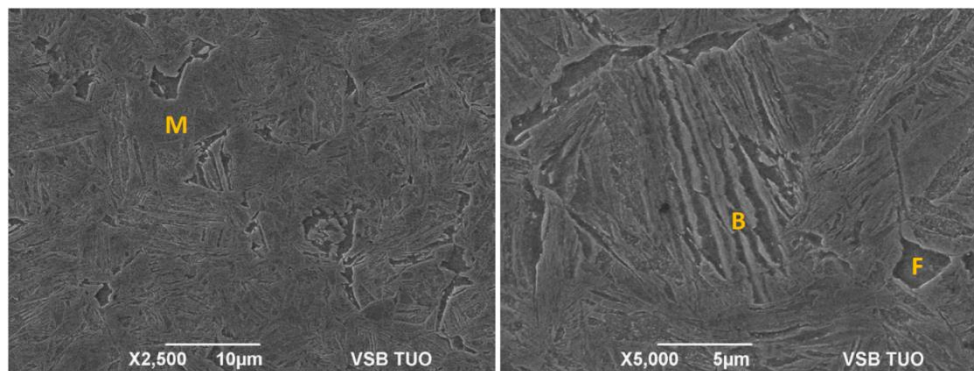
Cooling rate (°C·s ⁻¹)	Phase composition	Hardness HV 30	Cooling rate (°C·s ⁻¹)	Phase composition	Hardness HV 30
0.1	F+P	175	7.0	M+B+F	378
0.4	F+P	191	9.0	M+B+(F)	396
0.7	F+P+M+(B)	252	13	M+B+(F)	413
0.9	F+M+B+P	272	16	M+(B)+(F)	436
1.2	F+M+B+(P)	294	19	M+(B)+(F)	440
2.0	M+F+B	321	25	M+(B)+(F)	447
4.5	M+B+F	350	35	M+[F]+[B]	467



a) 0.4 °C·s⁻¹



b) 0.7 °C·s⁻¹



c) 35 °C·s⁻¹

Figure 4 Effect of cooling rate on the phase composition (SEM)

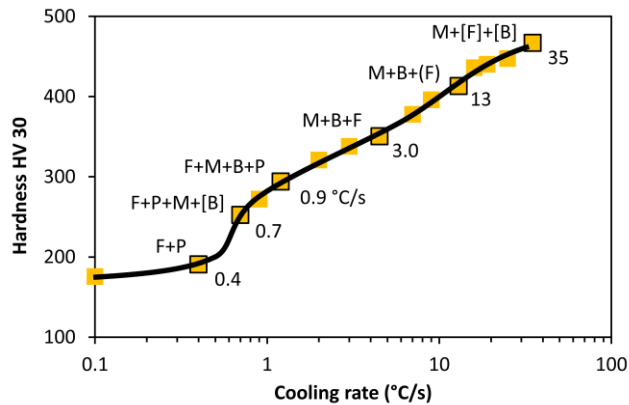
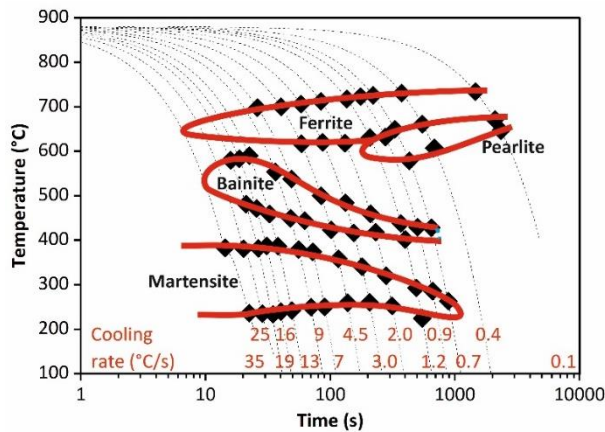
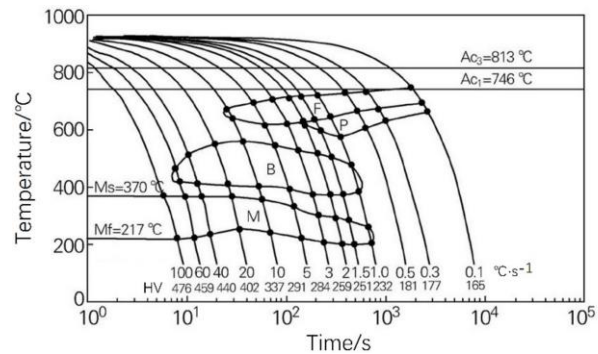


Figure 5 Hardness influenced by cooling rate



a) DCCT - this study



b) CCT - published in [6]

Figure 6 CCT diagrams of steel 20MnCrS5

In the DCCT diagram constructed for the similar steel and deformation conditions but from a lower austenitization temperature of 850 °C [9], the nose of the start of the ferritic and pearlitic transformation is significantly shifted to the longer times. This contradicts the results of previous studies, e.g. [4,10], that a lower austenitizing temperature with a shorter duration accelerates diffusion-controlled transformations. This anomaly can be explained by the possible effect of a different chemical composition with a higher content of elements such as Cr, Mo, Mn, Ni or B [4,9,10].

Another study [11] compiled a CCT diagram (without the influence of previous deformation) - see **Figure 6b**. The austenitizing temperature here was the same 880 °C. Apart from the elongated ferritic region, the curves in **Figures 6a** and **6b** are very similar. A comparison of experimentally obtained and literary data thus confirmed the significance of the austenitization temperature in dilatometric tests, respectively the influence of finish-rolling temperatures in operating conditions [4,10].

4. CONCLUSION

The DCCT diagram of 20MnCrS5 steel was constructed based on a high number of dilatometric tests with the influence of previous deformation after 880 °C austenitization. The key finding is that up to a cooling rate of 0.4 °C·s⁻¹, the structure of the steel consists only of ferrite and pearlite. In the investigated steel, certain occurrence of martensite and bainite already occurs at a cooling rate of 0.7 °C·s⁻¹. At the highest cooling rate of 35 °C·s⁻¹, the structure of the steel is almost purely martensitic with trace amounts of ferrite and bainite.

ACKNOWLEDGEMENTS

This article was created with the contribution of the Student grant competition project SP2023/049 “The influence of production parameters and operating conditions on the microstructure and utility properties of metallic materials” (VSB-TUO). The authors would like to thank Dr. K. Konečná for taking the SEM images of the microstructures.

REFERENCES

- [1] ELZANATY, H. Effect of Carburization on the Mechanical Properties of the Mild Steel. *International Journal of Innovation and Applied Studies*. 2014, vol. 6, pp. 987-994. ISSN 2028-9324.
- [2] LIU, S.K., YANG, L., ZHU, D.G., ZHANG, J. The influence of the alloying elements upon the transformation kinetics and morphologies of ferrite plates in alloy steels. *Metall. Mater. Trans. A*. 1994, vol. 25, pp. 1991-2000, Available from: <https://doi.org/10.1007/BF02649047>.
- [3] CALVO, J., JUNG, I.H., ELWAZRI, A.M., BAI, D., YUE, S. Influence of the chemical composition on transformation behaviour of low carbon microalloyed steels. *J. Mater. Sci. Eng. A*. 2009, vol. 520, pp. 90-96, Available from: <https://doi.org/10.1016/j.msea.2009.05.027>.
- [4] ŠEVČÁK, V., BENČ, M., KAWULOK, R., KAWULOK, P., SCHINDLER, I., OPĚLA, P., TUROŇOVÁ, P. Study of Effect of Deformation and High-temperature Austenitization on the Transformation Kinetics of P620Q steel. (in Czech). *Hutnické listy*. 2018, vol. 71, no. 6, pp. 23-28. ISSN 0018-8069.
- [5] KHLESTOV, V.M., KONOPLEVA, E.V., MCQUEEN, H.J. Effects of deformation and heating temperature on the austenite transformation to pearlite in high alloy tool steels. *Mater. Sci. Technol*. 2002, vol. 18, pp. 54-60, Available from: <https://doi.org/10.1179/026708301125000212>.
- [6] ARANDA, M. M., KIM, B., REMENTERIA, R., CAPDEVILA, C., GARCÍA DE ANDRES, C. Effect of prior austenite grain size on pearlite transformation in a hypo-eutectoid Fe-C-Mn steel. *Metall. Mater. Trans. A*. 2014, vol. 45, pp. 1778-1786. Available from: <https://doi.org/10.1007/s11661-013-1996-0>.
- [7] GRAJCAR, A., MORAWIEC, M., ZALECKI, W. Austenite Decomposition and Precipitation Behavior of Plastically Deformed Low-Si Microalloyed Steel. *Metals*. 2018, vol. 8, Article number 1028. Available from: <https://doi.org/10.3390/met8121028>.
- [8] YIN, S.B., SUN, X.J., LIU, Q.Y., ZHANG, Z.B. Influence of Deformation on Transformation of Low-Carbon and High Nb-Containing Steel during Continuous Cooling. *J. Iron Steel Res. Int*. 2010, vol. 17, pp. 43-47. Available from: [https://doi.org/10.1016/S1006-706X\(10\)60057-X](https://doi.org/10.1016/S1006-706X(10)60057-X).
- [9] KAWULOK, R., KAWULOK, P., SCHINDLER, I., OPĚLA, P., RUSZ, S., ŠEVČÁK, V., SOLOWSKI, Z. Study of the effect of deformation on transformation diagrams of two low-alloy manganese-chromium steels. *Archives of Metallurgy and Materials*. 2018, vol. 63, no. 4, pp. 1735-1741. ISSN 2300-1909. Available from: <https://doi.org/10.24425/amm.2018.125099>.
- [10] BENAROSCH, A., MARINI, B., TOFFOLON-MASCLET, C., TRZASKA, Z., MESLIN, E., GUILLOT, I. Effect of cooling rate on the microstructures of three low carbon alloys with different manganese and molybdenum contents. *Metallurgical Research & Technology*. 2022, vol. 119, Article number 520. Available from: <https://doi.org/10.1051/metal/2022059>.
- [11] LIANG, X., LI, X.J., LIN X.Y., FAN, Z.Y., LUO, P., SUN, F.L., GAO, B.K., ZHOU, T., DU Q.N., XIE, H.S. The Effect on Carburizing Process on Microstructure and Properties of 20MnCr5 Gear Steel. *Journal of Physics: Conference Series*. 2021, vol. 1885. Available from: <https://doi.org/10.1088/1742-6596/1885/2/022024>.